FULL PAPER

Thin, Deformable, and Safety-Reinforced Plastic Crystal Polymer Electrolytes for High-Performance Flexible Lithium-Ion Batteries

*Keun-Ho Choi, Sung-Ju Cho, Se-Hee Kim, Yo Han Kwon, Je Young Kim, and Sang-Young Lee**

A new class of highly thin, deformable, and safety-reinforced plastic crystal polymer electrolytes (N-PCPEs) is demonstrated as an innovative solid electrolyte for potential use in high-performance flexible lithium-ion batteries with aesthetic versatility and robust safety. The unusual N-PCPEs are fabricated by combining a plastic crystal polymer electrolyte with a porous polyethylene terephthalate (PET) nonwoven. Herein, the three-dimensional reticulated plastic crystal polymer electrolyte matrix is formed directly inside the PET nonwoven skeleton via in-situ UV-crosslinking of ethoxylated trimethylolpropane triacrylate (ETPTA) monomer, under co-presence of plastic crystal electrolyte. The PET nonwoven is incorporated as a compliant skeleton to enhance mechanical/dimensional strength of N-PCPE. Owing to this structural uniqueness, the N-PCPE shows significant improvements in the film thickness and deformability with maintaining advantageous features (such as high ionic conductivity and thermal stability) of the PCE. Based on structural/physicochemical characterization of N-PCPE, its potential application as a solid electrolyte for flexible lithium-ion batteries is explored by scrutinizing the electrochemical performance of cells. The high ionic conductance of N-PCPE, along with its excellent deformability, plays a viable role in improving cell performance (particularly at high current densities and also mechanically deformed states). Notably, the cell assembled with N-PCPE exhibits stable electrochemical performance even under a severely wrinkled state, without suffering from internal short-circuit failures between electrodes.

1. Introduction

As the scientific/industrial importance of user-tailored, various sized/shaped mobile electronic devices, including shape-conformable portable wireless gadgets, roll-up displays, and wearable/patchable electronics, is rapidly growing, flexible lithium-ion batteries with aesthetic diversity and unique functionality garner increasing attention as a promising power source.[1–8] In the development of the flexible batteries, the lack of variety in their shape imposes stringent limitations on achieving a satisfactory level of architectural flexibility. Another formidable challenge to be urgently resolved is how to ensure cell safety because a large extent of mechanical deformation that is commonly exerted on flexible batteries is likely to trigger internal short-circuit failures between electrodes, resulting in unwanted fire or explosion of cells.

From the viewpoint of material breakthrough for the realization of full-fledged flexible batteries affording high performance and robust safety, design/synthesis of readily-deformable solid electrolytes, in addition to research activities on advanced electrode materials with reliable attributes, is demanded with higher priority to secure a wide range of form factors that allow facile integration into differently shaped batteries without provoking safety concerns.[9–16]

One radical attempt to fabricate advanced solid electrolytes that can fulfill the abovementioned requirements is the exploitation of low melting point ionic conductors such as plastic crystal electrolytes (PCEs). The PCEs, which are composed of lithium salts and plastic crystals bearing good solvation capability, are characterized with unusual thermal stability and ionic transport behavior.[17–26] Succinonitrile (SN, NC–CH_2–CH_2–CN) is a representative organic matrix showing plastic crystal behavior with a plastic crystalline phase in temperature range between around –40 °C (a transition temperature from crystalline to plastic crystalline phase) to 60 °C (from plastic crystalline phase to melted state).[19,20] Due to the presence of trans-gauche isomerism involving rotation of molecules about central C–C bonds of SN, SN/lithium salt-based PCEs provide high ionic conductivity more than 10^{-3} S cm^{-1} at room temperature. Another salient benefit of the PCEs is the superior thermal

K.-H. Choi, S.-J. Cho, S.-H. Kim, Prof. S.-Y. Lee
Interdisciplinary School of Green Energy
Ulsan National Institute of Science and Technology (UNIST)
Ulsan, 689-798, Korea
E-mail: syleek@unist.ac.kr
Y. H. Kwon, J. Y. Kim
Batteries R&D
LG Chem
Yusong-gu, Daejon, 305-380, Korea

DOI: 10.1002/adfm.201301345

stability (negligibly volatile up to 150 °C) and nonflammability,[19,25] as compared to conventional volatile and flammable carbonate-based liquid electrolytes that are believed to be crucially responsible for safety problems of cells. Despite of these advantageous characteristics, the application of the PCEs to flexible batteries is staggered due to their poor mechanical properties. In general, the PCEs are excessively plastic and show liquid-like behavior at room temperature.

In an effort to overcome these shortcomings of the PCEs, the combination with a polymer matrix, leading to a plastic crystal polymer electrolyte (more specifically, PCE/polymer matrix-based gel polymer electrolyte, PCPE), has been extensively investigated.[21–26] Although the PCPE-based approaches are effective in improving the mechanical strength and rigidity of PCEs, most PCPEs are still struggling with insufficient mechanical flexibility. In addition, the PCPE films are too thick in what their another important role as a separator membrane is concerned (in most cases, more than 100 μm), thereby exerting a detrimental influence on ionic transport via PCPE films (in terms of ionic conductance) and also impairing volumetric energy density of cells (due to the loss of effective volume for electrodes). It is generally believed that ionic conductance ($G = (\sigma A)/l$, where σ is the ionic conductivity, A is the sample area, and l is the sample thickness) of polymer electrolytes is more important than their ionic conductivity, which is normalized by the thickness of the film.[27] For instance, a thick polymer electrolyte tends to offer long path for ionic diffusion (resulting in low ionic conductance), giving rise to an increase in Ohmic polarization (i.e., IR drop) of cells. As a consequence, the cell performance is deteriorated, notably becoming more pronounced at higher current densities. Therefore, the thickness reduction of PCPE films, along with attaining their deformability, is a critical prerequisite for facilitating their successful application in flexible lithium-ion batteries.

In the present study, as a facile and scalable strategy to resolve the abovementioned drawbacks of typical PCPEs and also to fulfill the aforementioned stringent requirements for full-fledged flexible lithium-ion batteries, we demonstrate a new class of highly thin, deformable, and safety-reinforced PCPEs (denoted as "N-PCPEs"). Herein, a polyethylene terephthalate (PET) nonwoven is incorporated as a compliant skeleton to improve mechanical properties (in particular, film thickness and deformability) of the N-PCPE. The three-dimensional reticulated plastic crystal polymer electrolyte matrix is formed directly inside the PET nonwoven skeleton via in-situ UV-crosslinking of ethoxylated trimethylolpropane triacrylate (ETPTA) monomer under the co-presence of PCE (=1 M lithium *bis*-trifluoromethanesulphonimide (LiTFSI) in SN). The beneficial contribution of the UV-crosslinked ETPTA polymer to lithium ion-conductive polymer electrolytes was demonstrated in our previous publications.[12,24,25]

Meanwhile, a structural design concept exploiting a porous substrate as a mechanical framework for fabrication of composite polymer electrolytes was introduced in previous work.[28–30] However, to date, no relevant studies have been reported in the case of PCEs. More notably, combination of compliant PET nonwoven skeleton with PCE/UV-crosslinked polymer matrix, to the best of our knowledge, is the first attempt in the development of PCPE systems. Owing to this unique structural integrity, the N-PCPE exhibits remarkable improvement in film thickness and mechanical flexibility, without impairing advantageous features (such as high ionic conductivity and thermal stability) of PCEs.

Based on the structural/physicochemical characterization (more specifically, chemical structures, morphology, deformability, and ionic conductance) of the N-PCPE, its potential application as a new solid electrolyte for flexible lithium-ion batteries is explored by analyzing cell performance (particularly at high current densities). Moreover, the electrochemical performance and internal short-circuit behavior of cells under physically deformed states are quantitatively characterized as a function of bending radius of cells. Finally, the electrochemical activity of a severely wrinkled cell is examined by monitoring the variation in cell voltage and charge/discharge behaviors. These results of the N-PCPEs are compared with those of a control PCPE (denoted as "X-PCPE") solely containing PCE/UV-crosslinked ETPTA polymer matrix without the PET nonwoven skeleton.

2. Results and Discussion

2.1. Unique Characteristics of N-PCPE as a Thin, Deformable, and Safety-Reinforced Solid Electrolyte

Unique characteristics of N-PCPE as a thin, deformable, and safety-reinforced solid electrolyte were investigated in great detail. A porous PET nonwoven (thickness ≈13 μm) is composed of multi-fibrous layers having large-sized pores (approximately more than 5 μm) irregularly formed between the micro-diameter fibers (Figure S1, Supporting Information). Meanwhile, the morphological analysis (cross-sectional view, **Figure 1**a) of the N-PCPE shows that the PET porous nonwoven is well-impregnated with the plastic crystal polymer electrolyte matrix (PCE/UV-cured ETPTA polymer). Owing to this structural uniqueness, the N-PCPE allows the substantial reduction in the film thickness (≈25 μm) compared to the thick X-PCPE (≈210 μm) containing no PET nonwoven skeleton (Figure 1b). Here, it is of note that the substantially reduced film thickness enables the N-PCPE to impart higher ionic conductance and also contribute to higher volumetric energy density of cells (i.e., can potentially store larger amount of electrode materials in cells).

Ionic transport of N-PCPE is expected to strongly depend on porous structure of PET nonwoven skeleton, because the PET nonwoven itself is ionically nonconductive and, thus, ionic migration occurs exclusively via the impregnated, 3D reticulated plastic crystal polymer electrolyte matrix. More specifically, the interconnectivity and amount of plastic crystal polymer electrolyte matrix play critical roles in determining ionic conduction of N-PCPE. The morphological results (Figure 1) demonstrate that the three-dimensionally interconnected plastic crystal polymer electrolyte matrix is successfully formed in the N-PCPE owing to the highly porous structure (average porosity ≈70%) of the PET nonwoven skeleton. This well-developed interconnectivity of the plastic crystal polymer electrolyte matrix, in combination with the low film thickness, allows the N-PCPE to provide facile ionic transport, which will be further discussed in the following section.

In addition to this morphological characterization, the chemical structure and plastic crystal behavior of the N-PCPE were

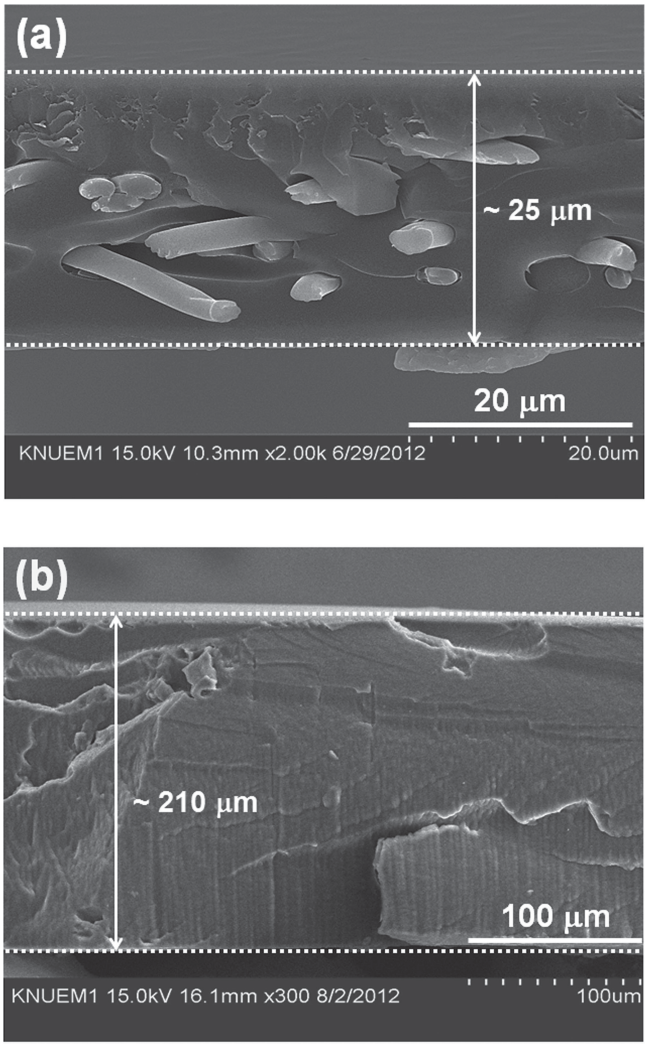

Figure 1. Morphological characterization (cross-sectional field emission scanning electron microscopy (FESEM) images) of: a) N-PCPE (thickness ≈25 μm) demonstrating the successful impregnation of plastic crystal polymer electrolyte matrix into PET nonwoven skeleton, b) X-PCPE (thickness ≈210 μm) containing no PET nonwoven skeleton.

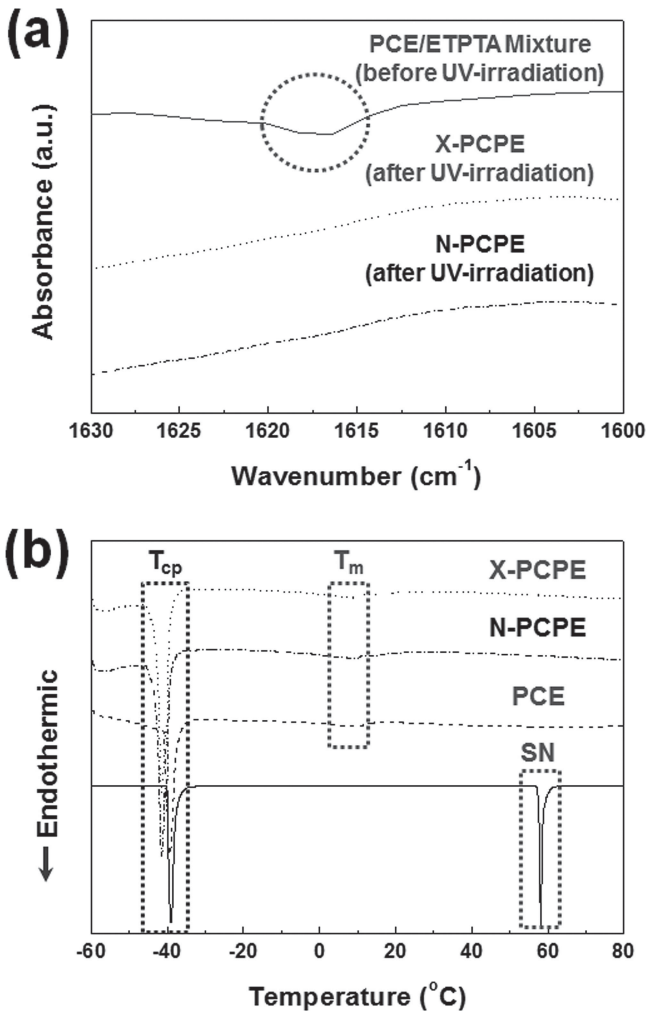

Figure 2. a) FTIR spectra of acrylic C=C double bonds of ETPTA in X-PCPE and N-PCPE, before/after UV-irradiation. b) DSC profiles showing plastic crystal behavior (i.e., transition temperatures, T_{cp} and T_m) of SN in pristine SN, PCE, X-PCPE, and N-PCPE.

elucidated. Firstly, the in-situ UV-crosslinking reaction of the N-PCPE was examined by monitoring the change in the Fourier transform infrared spectroscopy (FTIR) peaks[24,25] assigned to acrylic C=C bonds (1610–1625 cm^{-1}) of the ETPTA monomer before/after the UV-irradiation. **Figure 2**a shows that, after the UV-irradiation, the FTIR peaks of acrylic C=C bonds disappear at the N-PCPE as well as the X-PCPE, revealing that the ETPTA monomer is successfully photopolymerized under the presence of the PCE and also PET nonwoven skeleton. The crosslinking reaction of the N-PCPE was also characterized by measuring its gel content. The gel content (i.e., insoluble polymer fraction after solvent (dimethyl carbonate and acetone) extraction) of the N-PCPE and also X-PCPE was found to be more than 99%, verifying that the crosslinked polymer was generated in both the PCPEs via the in-situ UV-curing reaction of the ETPTA monomer.

The plastic crystal behavior of the N-PCPE was elucidated by measuring the characteristic transition temperatures (here, T_{cp} is the transition temperature from crystal to plastic crystal phase and T_m is the melting peak temperature) of SN. Figure 2b shows that the two endothermic peaks corresponding to T_{cp} (≈ –39 °C) and T_m (≈10 °C) of SN are observed in the N-PCPE, which appear to be similar to those of the X-PCPE. This differential scanning calorimetry (DSC) result demonstrates that the plastic crystal behavior of the N-PCPE is not disrupted by the introduction of the PET nonwoven skeleton. More detailed characterization on the change in the characteristic transition temperatures of SN with incorporation of lithium salt and polymer matrix was conducted in the previous publications.[22–25]

Another distinctive feature of the N-PCPE is the thermal stability due to the presence of thermoresistant PCE. The thermogravimetric analysis (TGA) measurement (dynamic mode, heating rate = 10 °C min^{-1}) shows that typical carbonate-based liquid electrolyte (1 M LiTFSI in ethylene carbonate (EC)/dimethyl carbonate (DMC) = 1/1 v/v) yields significant weight loss even below 100 °C because of the low boiling temperature (≈90 °C) of DMC (Figure S2a, Supporting Information). In

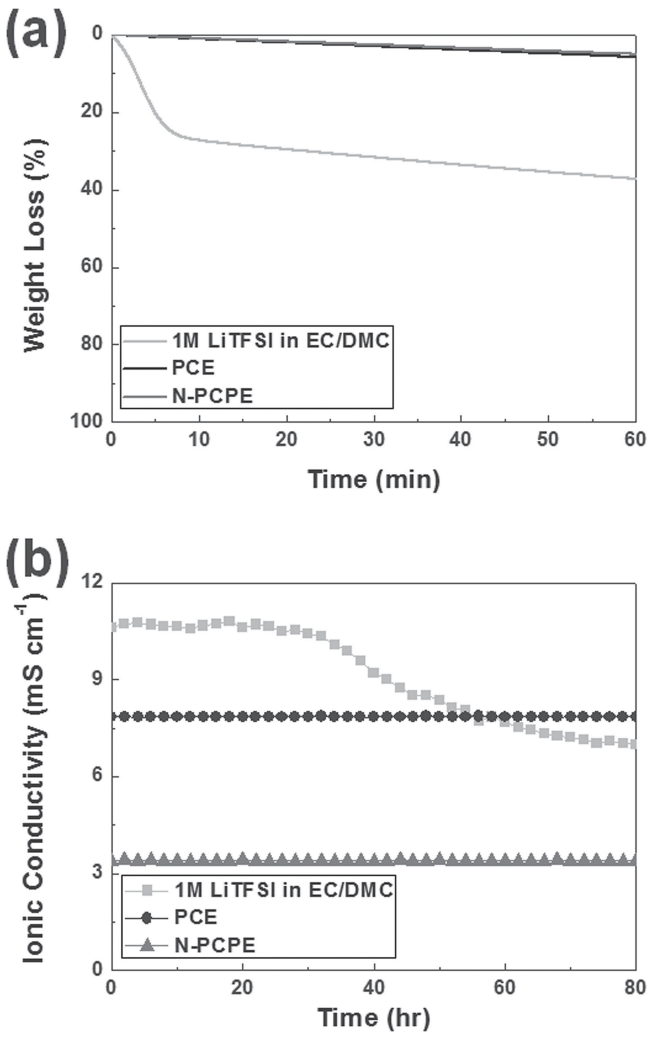

Figure 3. Thermal stability of PCE, N-PCPE, and conventional carbonate-based liquid electrolyte (1 M LiTFSI in EC/DMC = 1/1 v/v): a) TGA thermograms (isothermal mode at 80 °C) and b) time evolution of ionic conductivity at 80 °C.

contrast, the N-PCPE as well as PCE is negligibly volatile up to a high temperature of approximately 150 °C.

In order to further elucidate the unusual thermal stability of the N-PCPE, another TGA measurement based on an isothermal mode (at 80 °C) was carried out. The N-PCPE and PCE do not show any weight loss with elapsed time, whereas the EC/DMC-based liquid electrolyte rapidly loses its weight (**Figure 3**a). In addition, no appreciable difference in the TGA profiles was observed between the N-PCPE and PCE, indicating that the UV-cured ETPTA polymer and PET nonwoven skeleton do not impair the thermal characteristics of the PCE. This superior thermal stability of the N-PCPE is expected to play a viable role in achieving excellent ionic conductivity at high temperature. Figure 3b shows the time evolution of ionic conductivity of N-PCPE, PCE, and also EC/DMC-based liquid electrolyte at a high temperature of 80 °C. It is found that the ionic conductivity of the EC/DMC-based liquid electrolyte is higher than those of the N-PCPE and PCE, however, after 30 h, is sharply declined with time. On the other hand, no significant decrease in the ionic conductivity with elapsed time was found at the N-PCPE and PCE, which is well-consistent with the results of isothermal (at 80 °C) TGA measurement.

Thermal stability of electrolytes is known to be of great importance for securing cell safety, since highly volatile liquid electrolytes tend to trigger swelling of cells, often resulting in fire or explosion of cells.[31–34] The effect of electrolytes on cell swelling was investigated, where the cells charged at state of charge (SOC) of 50% were placed on a hot plate (set at 150 °C). As expected, the cell incorporating the volatile EC/DMC-based liquid electrolyte easily swells with time. In comparison, no detectable change in the cell dimension was observed at the N-PCPE or PCE (Figure S2b, Supporting Information). These results demonstrate that the N-PCPE can be suggested as a safety-reinforced solid electrolyte to outperform conventional volatile carbonate-based liquid electrolytes.

The temperature-dependent ionic conductivity of the N-PCPE is measured and also compared with that of the X-PCPE. **Figure 4**a shows that, over a wide range of temperatures, the

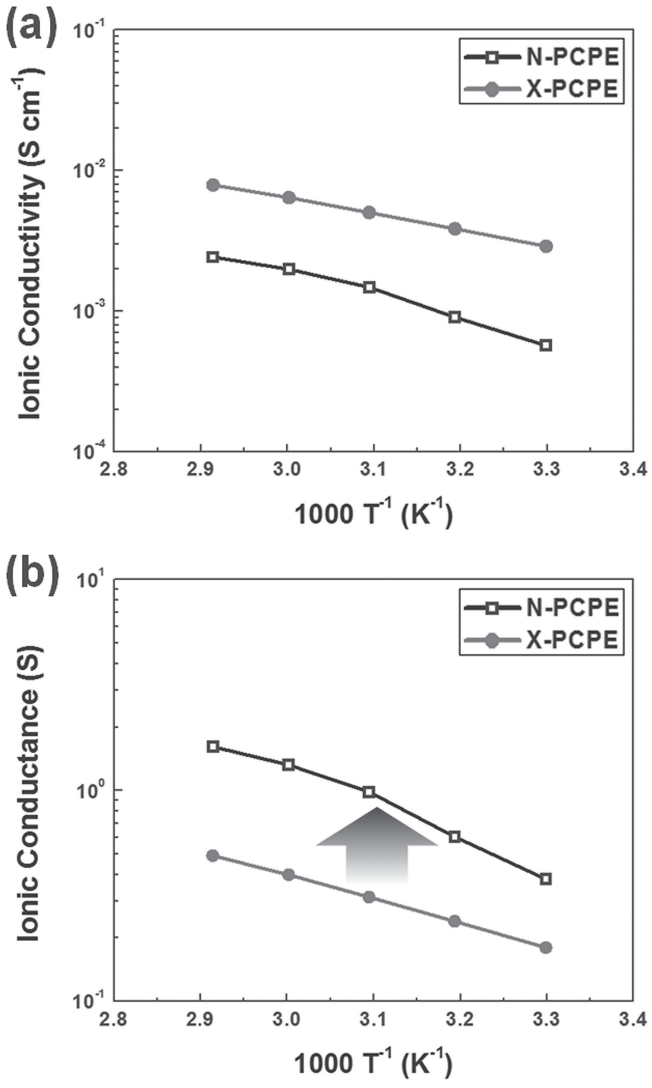

Figure 4. Comparison of ionic transport behavior between X-PCPE and N-PCPE as a function of temperature: a) ionic conductivity and b) ionic conductance.

N-PCPE presents the lower ionic conductivity than the X-PCPE. This decrease in the ionic conductivity of the N-PCPE is ascribed to the presence of the PET nonwoven skeleton. In the N-PCPE, ionic transport is allowed only through the impregnated plastic crystal polymer electrolyte matrix, because the PET nonwoven skeleton is ionically nonconductive. However, owing to the well-developed, 3D reticulated plastic crystal polymer electrolyte matrix, a satisfactory ionic conductivity (for example, 5.7×10^{-4} S cm^{-1} at 30 °C) is obtained at the N-PCPE.

Meanwhile, when practical application of polymer electrolytes (acting as an electrolyte and also separator membrane) to lithium-ion batteries is concerned, it should be noted that ionic conductance of polymer electrolytes is more important in determining cell performance, rather than ionic conductivity that is normalized by sample thickness.[27] For instance, thin polymer electrolytes are advantageous in delivering high ionic conductance (i.e., alleviating actual ionic resistance) due to short ion diffusion path. The previous morphological results (Figure 1) showed that the N-PCPE (≈25 μm) has the significantly lower film thickness than the X-PCPE (≈210 μm). Figure 4b underlines the advantageous effect of thin N-PCPE on the ionic conductance. Contrary to the results of ionic conductivity, the N-PCPE exhibits the higher ionic conductance than the X-PCPE. This higher ionic conductance of the N-PCPE is expected to beneficially influence cell performance, which will be discussed in great detail below.

The deformability of the N-PCPE is characterized by conducting bending cycle test, where the number of bending cycles (under longitudinal strain ranged from 10 to 30 mm) before mechanical breakdown of the samples quantitatively represents their deformability.[12,25] **Figure 5**a shows that, due to the incorporation of the UV-cured ETPTA polymer, both the X-PCPE and N-PCPE are self-standing even at a low concentration of polymer (PCE/UV-cured ETPTA polymer =85/15 w/w) and also exhibit strong tolerance to mechanical breakage upon appreciable bending stress. However, when they are subjected to the repeated bending, the X-PCPE is broken down just after the 3rd bending cycle (Figure 5b). By contrast, the N-PCPE retains its dimensional stability after the 50th bending cycle (Figure 5c). More notably, the microstructure (an inset image in Figure 5c) of N-PCPE is not disrupted after the 50th bending cycle. In addition, Figure 5d underlines that the N-PCPE is not mechanically ruptured after being fully folded at a bending angle of almost 180 ° and can be also wound several times along a glass rod (diameter =5 mm). These results demonstrate that the introduction of the PET nonwoven substrate as a compliant skeleton is an effective way to substantially improve the deformability of N-PCPE.

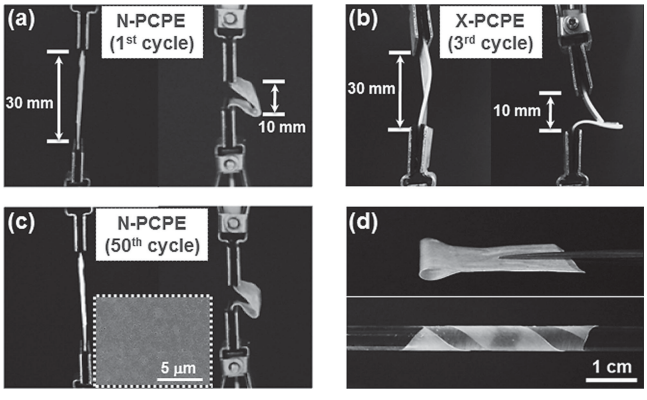

Figure 5. Mechanical bending test of: a) N-PCPE (after 1st bending cycle), b) X-PCPE (after 3rd bending cycle), c) N-PCPE (after 50th bending cycle) (an inset is a FESEM image depicting the microstructure of N-PCPE after 50th bending cycle), wherein samples are subjected to repeated bending stress until being mechanically ruptured at a strain rate of 10 mm min^{-1}. d) Photographs showing physical appearance of N-PCPE after being fully folded at a bending angle of almost 180 ° and also wound along a glass rod (diameter = 5 mm).

2.2. Potential Application of N-PCPE as a New Solid Electrolyte for Flexible Lithium-Ion Batteries, with a Focus on Cell Performance at High Current Densities and Mechanically Deformed States

The electrochemical performance of cells incorporating the N-PCPE was evaluated in terms of discharge capacity, discharge C-rate capability, and cyclability at various charge/discharge conditions and also mechanically deformed states. A cell assembly employed herein, composed of $LiCoO_2$, $Li_4Ti_5O_{12}$, and N-PCPE, is illustrated in **Figure 6**a, where the role of N-PCPE as a separator membrane as well as electrolyte is also demonstrated. The cell was charged at a constant current density of 0.1 C and discharged at various current densities ranged from 0.1 to 2.0 C under a voltage window of 1.5–2.7 V. Neither abnormal nor unstable discharge profiles were observed in the N-PCPE (Figure 6b) and X-PCPE (Figure 6c). The voltage and discharge capacity of cells gradually decrease with an increase of discharge current density, indicating the Ohmic polarization (i.e., IR drop) loss of cells. An intriguing finding is that the N-PCPE shows higher discharge capacities than the X-PCPE over a wide range of discharge current densities. This difference in the discharge capacities between the PCPEs becomes more noticeable at higher discharge current densities, where contribution of ionic transport to the Ohmic polarization is more influential.[35–37] Figure 6d summarizes the discharge capacities of the PCPEs as a function of discharge current density (i.e., discharge C-rate capability), revealing the superior discharge C-rate capability of the N-PCPE. This can be reasonably explained by considering ionic conductance of the PCPEs. The previous result (Figure 4b) showed that the N-PCPE (=0.38 S at 30 °C) presents the higher ionic conductance than the X-PCPE (=0.18 S at 30 °C) owing to the lower film thickness (i.e., shorter lithium-ion diffusion path). Hence, this facile ionic transport of the N-PCPE is expected to effectively alleviate the Ohmic polarization loss of cells, leading to the improvement of discharge capacities and also discharge C-rate capability.

The cycling performance of the N-PCPE was evaluated (**Figure 7**), where the cells were cycled at a constant charge/discharge current density (=0.2 C/0.2 C). The N-PCPE exhibits the superior charge/discharge capacity retention with cycling (Figure 7a), as compared to the X-PCPE showing gradual decrease in the charge/discharge capacities (Figure 7b). This improvement in the cycling performance of N-PCPE was summarized in Figure 7c. For example, discharge capacity

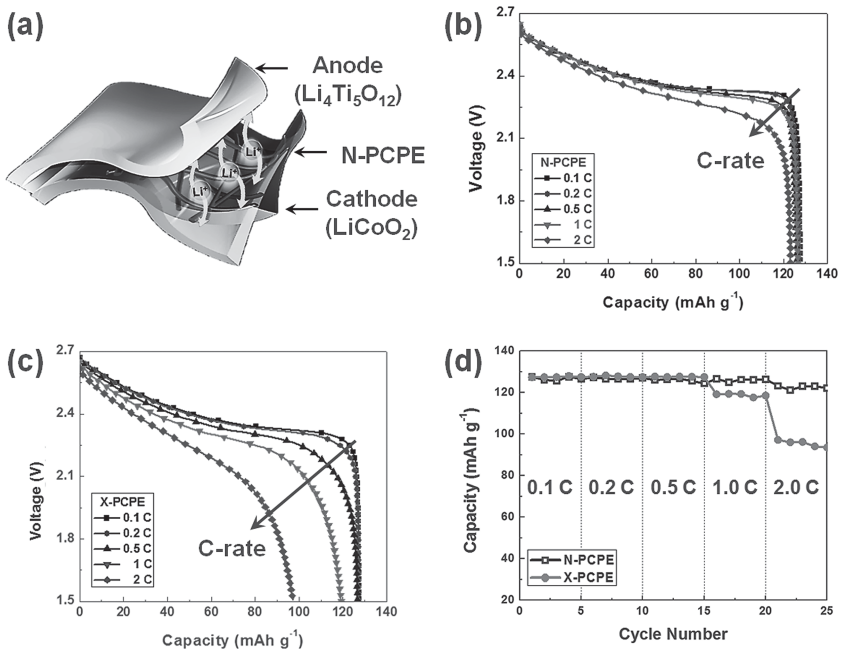

Figure 6. a) A schematic illustration of a cell assembly composed of $LiCoO_2$ (cathode), $Li_4Ti_5O_{12}$ (anode), and N-PCPE (acting as an electrolyte and separator membrane). Discharge profiles of cells (at different discharge current densities (from 0.1 to 2.0 C) assembled with: b) N-PCPE and c) X-PCPE. d) Comparison of discharge C-rate capability (i.e., discharge capacity as a function of discharge current density) between N-PCPE and X-PCPE.

retentions after the 50th cycle were ≈99% for the N-PCPE and ≈92% for the X-PCPE, respectively. Notably, the difference in the discharge capacity between the N-PCPE and X-PCPE becomes more pronounced at a higher charge/discharge current density (=1.0 C/1.0 C, Figure 7d), where the influence of IR drop on the cell capacity becomes more significant. This excellent cycling performance of the N-PCPE may be attributed to its high ionic conductance (Figure 5b), which possibly mitigates the Ohmic polarization of cells during cycling. In addition, it is reasonably speculated that the N-PCPE may have better interfacial contact with electrodes owing to its excellent flexibility,[12,25,26,38] thereby alleviating interfacial Ohmic resistance between the N-PCPE and electrodes during cycling.

In an effort to attain a more comprehensive understanding of the superior cycling performance of the N-PCPE, the AC impedance spectra of cells after the 1st and 50th cycle were analyzed (Figure S3, Supporting Information). This result demonstrates that the N-PCPE could offer good interfacial compatibility with electrodes during cycling,

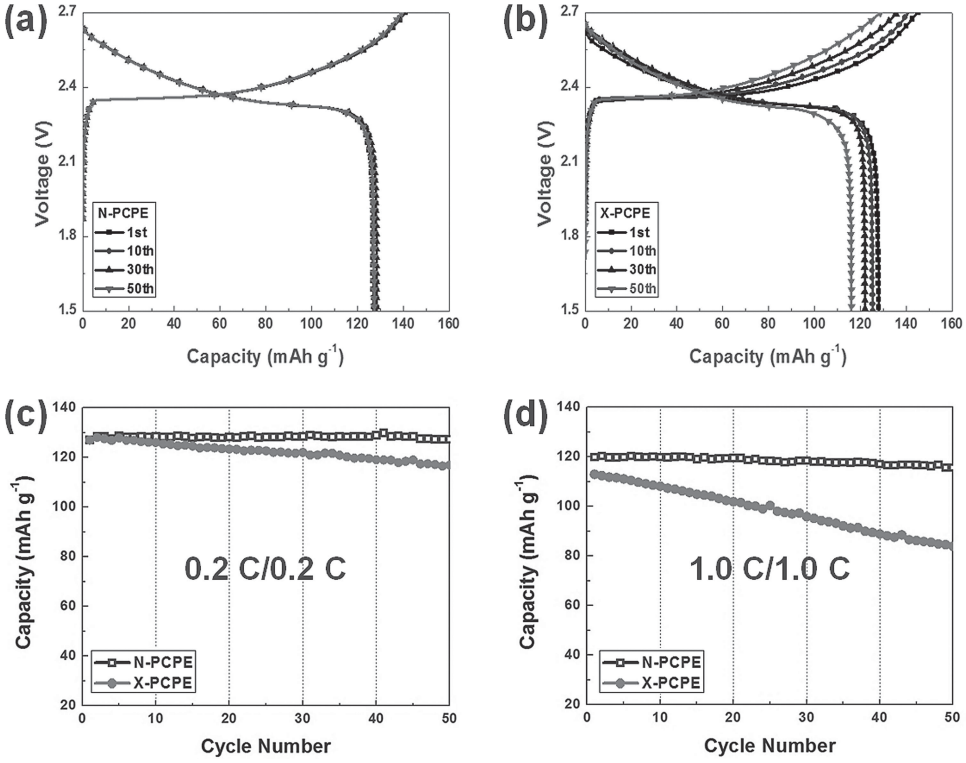

Figure 7. Variation in charge/discharge profiles of cells (=$LiCoO_2/Li_4Ti_5O_{12}$) during cycling at a charge/discharge current density of 0.2 C/0.2 C: a) N-PCPE and b) X-PCPE. Comparison of cycling performance (i.e., discharge capacity retention as a function of cycle number) between N-PCPE and X-PCPE at a charge/discharge current density of: c) 0.2 C/0.2 C and d) 1.0 C/1.0 C.

thereby contributing to the excellent cycling performance. More detailed discussion was described in the Supporting Information section.

Finally, in order to explore the applicability of N-PCPE to mechanically-deformable cells with shape versatility, aluminum pouch cells comprising $LiCoO_2$ (as a cathode), $Li_4Ti_5O_{12}$ (as an anode), and N-PCPE were fabricated and their cell performance was estimated as a function of mechanical deformation.[7,39] In these pouch cells, the N-PCPE should act as an electrolyte and also a separator membrane. In particular, as flexible batteries are vulnerable to internal short-circuit failures, mainly due to their serious shape deformation, the function of N-PCPE as a separator membrane that keeps electrical isolation between electrodes becomes more important.[40–43] This critical role of N-PCPE in the cell is conceptually illustrated in Figure 6a. **Figure 8**a shows that, under a normal static condition, the cells

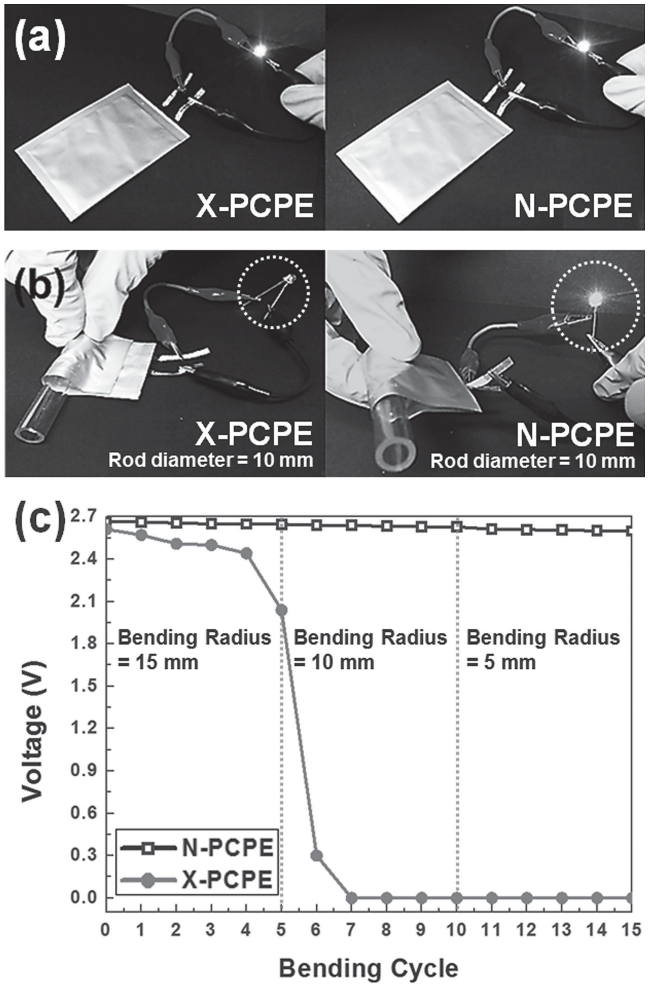

Figure 8. Applicability of N-PCPE to mechanically-deformed cells (aluminum pouch cells containing $LiCoO_2$/PCPE/$Li_4Ti_5O_{12}$ system). Photographs showing electrical state of red LED lamps connected to cells assembled with N-PCPE (or X-PCPE): a) under a normal static condition and b) under being manually bended 2 times along a glass rod (diameter = 10 mm). c) Variation in cell voltage during bending test as a function of bending cycle, where different-sized glass rods (diameter =5, 10, and 15 mm) are used in order to vary the deformed state of cells.

are successfully able to light up a red LED lamp. When the cells were manually bended 2 times along the glass rod (diameter =10 mm), the lamp of the cell incorporating the X-PCPE was extinguished (left side of Figure 8b). After this bending test, the cell voltage drops to zero, indicating that an internal short-circuit between electrodes occurs in the cell. In other words, the X-PCPE may be mechanically broken down and lose its basic function as a separator membrane preventing electrical short-circuit between the anode and cathode. On the other hand, the cell assembled with the N-PCPE continues to activate the lamp after being severely deformed (right side of Figure 8b). No electrical failure was observed even after the cell is repeatedly bended down to the glass rod more than 20th times. The cell voltage was in-situ monitored during the bending test as a function of bending cycle, where different-sized glass rods (diameter =5, 10, and 15 mm) were used in order to vary the deformed state of cells. Figure 8c shows that the cell assembled with the N-PCPE presents almost no loss in the voltage during the bending test, even after being bended several times along the small-sized glass rod (diameter =5 mm). In contrast, the cell voltage of the X-PCPE drops sharply just after the cell is bended along the mid-sized glass rod (diameter =10 mm). Here, it is worthwhile to note that the remarkably improved flexibility of cells incorporating the N-PCPE is consistent with the superior mechanical deformability of the N-PCPE (Figure 5).

Moreover, the cell assembled with the N-PCPE was extremely deformed and its electrochemical activity was investigated. **Figure 9**a shows that the lamp of the cell is still running even after the cell is severely wrinkled. In addition, cycling performance (charge/discharge current density =0.2 C/0.2 C) of the cell under this harsh measurement condition was estimated (Figure 9b). Notably, the cell exhibits very stable charge/discharge behavior with cycling (up to the 30th cycle). This is a solid evidence to prove that the N-PCPE shows unprecedented improvements in deformability and internal short-circuit prevention of cells.

3. Conclusions

The highly-thin, deformable, and safety-reinforced plastic crystal polymer electrolyte (N-PCPE) has been presented as a promising solid electrolyte for high-performance flexible lithium-ion batteries. The in-depth characterization of the morphology, FTIR peaks, and DSC/TGA thermograms of the N-PCPE demonstrated that the 3D reticulated plastic crystal polymer electrolyte matrix was successfully formed inside the compliant PET nonwoven skeleton without impairing the beneficial characteristics of the SN-based PCE. This structural uniqueness of the N-PCPE brought significant improvements in the film thickness and mechanical flexibility, as compared to the X-PCPE containing no PET nonwoven skeleton. Notably, the low film thickness of the N-PCPE contributed to improving ionic conductance and also potentially volumetric energy density of cells. This facile ionic transport of the N-PCPE, in combination with its excellent deformability, exerted beneficial influence on the cell performance (particularly at higher current densities). A remarkable finding of this study was that the cell incorporating the N-PCPE provided the stable electrochemical

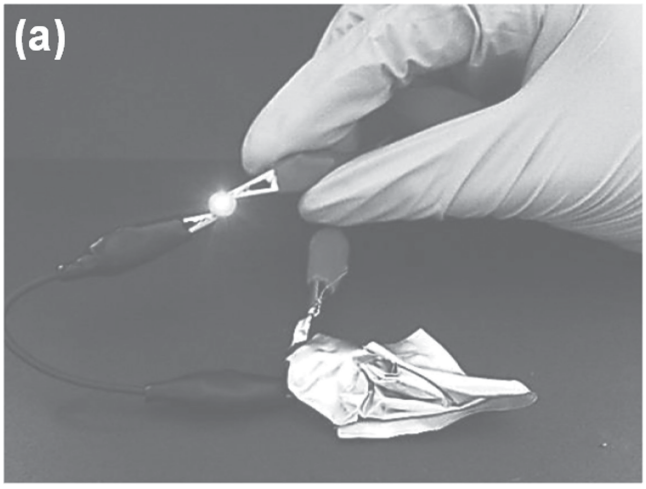

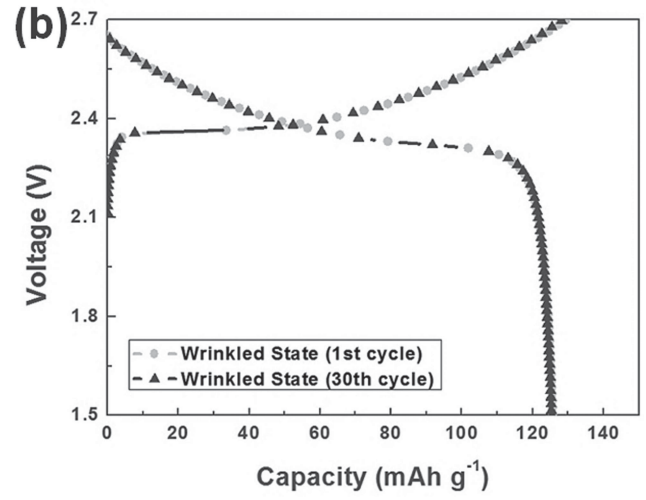

Figure 9. Applicability of N-PCPE to a severely wrinkled cell. a) A photograph showing active sate of a red LED lamp connected to the wrinkled cell assembled with N-PCPE. b) Charge/discharge profiles of the wrinkled cell with cycling (charge/discharge current density = 0.2 C/0.2 C).

performance without suffering from internal short-circuit problems under severely deformed states (even a wrinkled state). We believe that the exquisitely nanoarchitectured plastic crystal polymer electrolytes reported herein can be suggested as an advanced solid electrolyte to outperform conventional flammable carbonate-based liquid electrolytes and polyolefin separator membranes, thus facilitating successful development of high-performance flexible lithium-ion batteries with robust safety that are essentially needed as a suitable power source to boost the advent of next-generation mobile/wearable era.

4. Experimental Section

Fabrication of Plastic Crystal Polymer Electrolytes (N-PCPE and X-PCPE): For the fabrication of PCPEs, the ETPTA monomer was added into the PCE, where the PCE was prepared by adding 1 M LiTFSI into SN melted at 60 °C. The weight-based composition ratio of the PCE/ETPTA monomer was 85/15 (w/w), wherein the concentration of 2-hydroxy-2-methyl-1-phenyl-1-propanone (HMPP, photo-initiator) was 0.1 wt% of ETPTA monomer.[24–26] The chemical structure and physical appearance of the major components are displayed in **Scheme 1**. A wet-laid PET nonwoven substrate (average thickness =13 µm, Mitsubishi) was chosen as a compliant skeleton for the N-PCPE. The PET nonwoven was dipped into the PCE/ETPTA mixture solution and subjected to Meyer bar coating in order to achieve uniform thickness. The PCE/ETPTA mixture-immersed PET nonwoven was then exposed to UV-irradiation for 20 s. The UV-curing was performed using a Hg UV lamp (Lichtzen), with an irradiation peak intensity of approximately 2000 mW cm^{-2} on the sample surface. The thickness of the resulting N-PCPE was approximately 25 µm. All preparation procedures of both PCPEs were carried out in an argon-filled glove box. Meanwhile, the X-PCPE (a control sample) was fabricated by adopting the same materials and procedure as used for the preparation of the N-PCPE, except for solely using ETPTA as a polymer matrix without incorporating the PET nonwoven skeleton. A schematic illustration depicting the UV polymerization-assisted fabrication process, along with a photograph showing the mechanical bendability of the N-PCPE, is provided in Scheme 1.

Characterization of Physicochemical Properties and Electrochemical Performance of Plastic Crystal Polymer Electrolytes (N-PCPE and X-PCPE): The UV-crosslinking reaction of the PCPEs was investigated using a FTIR spectrometer (FT-3000, Excalibur) with a spectral resolution of 4 cm^{-1}. The gel content of the PCPEs was estimated by measuring the weight loss of the samples after being solvent-extracted in dimethyl carbonate

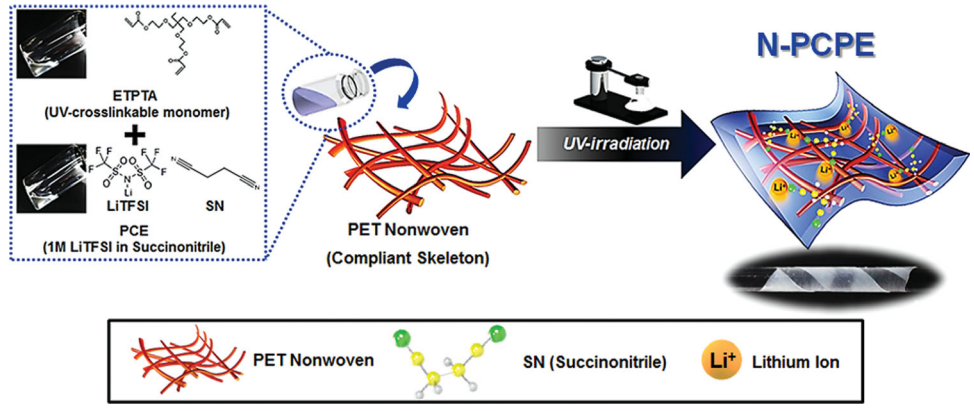

Scheme 1. A schematic illustration of UV polymerization-assisted fabrication process and chemical structure of N-PCPE (plastic crystal polymer electrolyte matrix combined with compliant PET nonwoven skeleton), along with a photograph showing mechanical flexibility of N-PCPE.

at 70 °C for 8 h and subsequently in acetone at room temperature for 24 h.[24–26] The cross-sectional morphology of the PCPEs was examined using a field emission scanning electron microscope (FESEM, S-4300, Hitachi). The mechanical flexibility of the PCPEs was evaluated via a bending test using a universal tensile tester (Lloyd LR 10K, Lloyd Instruments), where samples were deformed by repeated bending stress until being mechanically ruptured at a strain rate of 10 mm min^{-1}.[25] Here, the number of bending cycles before breakdown of the PCPEs quantitatively represents their mechanical deformability. In addition, the deformability of the samples was further characterized after being wound around cylindrical glass rods (diameter =5 mm). The ionic conductivity (σ) of the PCPEs was obtained using an impedance analyzer (VSP classic, Bio-Logic) over a frequency range of 1 to 10^6 Hz under a temperature range of 30 to 70 °C. Meanwhile, the ionic conductance (G) of the PCPEs was then calculated using an equation of $G = (\sigma A)/l$, where A is surface area of the PCPEs, and l is thickness of the PCPEs.

For evaluation of cell performance, a unit cell (2032-type coin) was assembled by sandwiching the PCCEs between a PCE-soaked $LiCoO_2$ cathode ($LiCoO_2$/PVdF binder/Super-P = 95/3/2 w/w/w) and a PCE-soaked $Li_4Ti_5O_{12}$ anode ($Li_4Ti_5O_{12}$/PVdF binder/Super-P = 88/10/2 w/w/w). The discharge capacities, discharge C-rate capability, and cyclability of the cells were estimated using battery test equipment (PNE Solution). The discharge capacities and C-rate capability were investigated by varying discharge current densities (i.e., discharge C-rates) from 0.1 (=0.1 mA cm^{-2}) to 2.0 C (=2 mA cm^{-2}) at a constant charge current density of 0.1 C under a voltage range of 1.5–2.7 V. The cells were cycled at a constant charge/discharge current density of 0.2 C/0.2 C and also 1.0 C/1.0 C. The time evolution of AC impedance of fully charged cells during cycling was monitored using the impedance analyzer over a frequency range of 10^{-2} to 10^6 Hz.

Supporting Information

Supporting Information is available from the Wiley Online Library or from the author.

Acknowledgements

This research was supported by the Converging Research Center Program through the Ministry of Education, Science and Technology (2012K001254). This work was also supported by Energy Efficiency and Resources R&D program (20112010100150) under the Ministry of Knowledge Economy, Republic of Korea.

Received: April 20, 2013
Revised: May 21, 2013
Published online: July 5, 2013

[1] B. Scrosati, *Nat. Nanotechnol.* **2007**, *2*, 598.
[2] H. Nishide, K. Oyaizu, *Science* **2008**, *319*, 737.
[3] S. Xu, Y. Zhang, J. Cho, J. Lee, X. Huang, L. Lia, J. A. Fan, Y. Su, J. Su, H. Zhang, H. Cheng, B. Lu, C. Yu, C. Chuang, T. Kim, T. Song, K. Shigeta, S. Kang, C. Dadgeviren, I. Petrov, P. Braun, Y. Huang, U. Paik, J. A. Rogers, *Nat. Commun.* **2013**, *4*, 1543.
[4] V. L. Pushparaj, M. M. Shaijumon, A. Kumar, S. Murugesan, L. Ci, R. Vajtai, R. J. Linhardt, O. Nalamasu, P. M. Ajayan, *Proc. Natl. Acad. Sci. U.S.A.* **2007**, *104*, 13574.
[5] G. Nystrom, A. Razaq, M. Stromme, L. Nyholm, A. Miharnyan, *Nano Lett.* **2009**, *9*, 3635.
[6] L. Hu, Y. Cui, *Energy Environ. Sci.* **2010**, *5*, 6423.
[7] Y. H. Kwon, S. W. Woo, H. R. Lee, H. K. Yu, K. T. Kim, B. H. Oh, S. Ahn, S. Y. Lee, S. W. Song, J. Cho, H. C. Shin, J. Y. Kim, *Adv. Mater.* **2012**, *24*, 5192.
[8] K. Wang, S. Luo, Y. Wu, X. He, F. Zhao, J. Wang, K. Jiang, S. Fan, *Adv. Funct. Mater.* **2013**, *23*, 846.
[9] A. Hammami, N. Raymond, M. Armand, *Nature* **2003**, *424*, 635.
[10] C. Masquelier, *Nat. Mater.* **2011**, *10*, 649.
[11] J. F. Ihlefeld, P. G. Clem, B. L. Doyle, P. G. Kotula, K. R. Fenton, A. Apblett, *Adv. Mater.* **2011**, *23*, 5663.
[12] E. H. Kil, K. H. Choi, H. J. Ha, S. Xu, J. A. Rogers, M. R. Kim, Y. G. Lee, K. M. Kim, K. Y. Cho, S. Y. Lee, *Adv. Mater.* **2013**, *25*, 1395.
[13] M. Palacin, *Chem. Soc. Rev.* **2009**, *38*, 2565.
[14] S. Wada, S. Kuroki, M. Nogami, *Energy Environ. Sci.* **2010**, *3*, 1995.
[15] V. L. Pushparaj, M. M. Shaijumon, A. Kumar, S. Murugesan, L. Ci, R. Vajtai, R. J. Linhardt, O. Nalamasu, P. M. Ajayan, *Proc. Natl. Acad. Sci. U.S.A.* **2007**, *104*, 13574.
[16] F. Liu, S. Song, D. Xue, H. Zhang, *Adv. Mater.* **2012**, *24*, 1089.
[17] D. MacFarlane, J. Huang, M. Forsyth, *Nature* **1999**, *402*, 792.
[18] S. Long, D. MacFarlane, M. Forsyth, *Solid State Ionics* **2003**, *161*, 105.
[19] P. Alarco, Y. Lebdeh, A. Abouimrane, M. Armand, *Nat. Mater.* **2004**, *3*, 476.
[20] S. Das, S. Prathapa, P. Menezes, T. Row, A. Bhattacharyya, *J. Phys. Chem. B* **2009**, *113*, 5025.
[21] L. Fan, J. Maier, *Electrochem. Commun.* **2006**, *8*, 1753.
[22] L. Fan, Y. Hu, A. Bhattacharyya, J. Maier, *Adv. Funct. Mater.* **2007**, *17*, 2800.
[23] M. Patel, K. Chandrappa, A. Bhattacharyya, *Electrochim. Acta* **2008**, *54*, 209.
[24] H. J. Ha, Y. H. Kwon, J. Y. Kim, S. Y. Lee, *Electrochim. Acta* **2011**, *57*, 40.
[25] H. J. Ha, E. H. Kil, Y. H. Kwon, J. Y. Kim, C. K. Lee, S. Y. Lee, *Energy Environ. Sci.* **2012**, *5*, 6491.
[26] K. H. Choi, S. H. Kim, H. J. Ha, E. H. Kil, C. K. Lee, S. B. Lee, J. K. Shim, S. Y. Lee, *J. Mater. Chem. A* **2013**, *1*, 5224.
[27] H. S. Jeong, S. Y. Lee, *J. Power Sources* **2011**, *196*, 6716.
[28] J. R. Nair, A. Chiappone, C. Gerbaldi, V. S. Ijeri, E. Zeno, R. Bongiovanni, S. Bodoardo, N. Penazzi, *Electrochim. Acta* **2011**, *57*, 104.
[29] J. R. Nair, C. Gerbaldi, A. Chiappone, E. Zeno, R. Bongiovanni, S. Bodoardo, N. Penazzi, *Electrochem. Commun.* **2009**, *11*, 1796.
[30] L. Wang, B. L. Yi, H. M. Zhang, Y. H. Liu, D. M. Xing, Z. G. Shao, Y. H. Cai, *J. Power Sources* **2007**, *167*, 47.
[31] R. V. Morford, D. T. Welna, C. E. Kellam, M. A. Hofmann, H. R. Allcock, *Solid State Ionics* **2006**, *177*, 721.
[32] H. P. Zhang, Q. Xia, B. Wang, L. C. Yang, Y. P. Wu, D. I. Sun, C. I. Gan, H. J. Luo, A. W. Bebeda, T. V. Ree, *Electrochem. Commun.* **2009**, *11*, 526.
[33] S. V. Sazhin, M. K. Harrup, K. L. Gering, *J. Power Sources* **2011**, *196*, 3433.
[34] C. Arbizzani, G. Gabrielli, M. Mastragostino, *J. Power Sources* **2011**, *196*, 4801.
[35] E. S. Choi, S. Y. Lee, *J. Mater. Chem.* **2011**, *21*, 14747.
[36] J. H. Cho, J. H. Park, M. H. Lee, H. G. Song, S. Y. Lee, *Energy Environ. Sci.* **2012**, *5*, 7124.
[37] Y. K. Sun, Z. Chen, H. J. Noh, D. J. Lee, H. G. Jung, Y. Ren, S. Wang, C. S. Yoon, S. T. Myung, K. Amine, *Nat. Mater.* **2012**, *11*, 942.
[38] S. H. Kim, K. H. Choi, S. J. Cho, E. H. Kil, S. Y. Lee, *J. Mater. Chem. A* **2013**, *1*, 4949.
[39] M. Koo, K. I. Park, S. H. Lee, M. Suh, D. Y. Jeon, J. W. Choi, K. Kang, K. J. Lee, *Nano Lett.* **2012**, *12*, 4810.
[40] M. Rosso, C. Brissot, A. Teyssot, M. Dolle, L. Sannier, J. M. Tarascon, R. Bouchet, S. Lascaud, *Electrochim. Acta* **2006**, *51*, 5334.
[41] S. Liu, N. Imanishi, T. Zhang, A. Hirano, Y. Takeda, O. Yamamoto, *J. Power Sources* **2010**, *195*, 6847.
[42] P. Arora, Z. Zhang, *Chem. Rev.* **2004**, *104*, 4419.
[43] C. J. Orendorff, T. N. Lambert, C. A. Chavez, M. Bencomo, K. R. Fenton, *Adv. Energy Mater.* **2013**, *3*, 314.